

# Developing GaN HEMTs for Ka-Band with 20W

Kazutaka Takagi#, Keiichi Matsushita#, Yasushi Kashiwabara#, Kazutoshi Masuda#, Shinichiro Nakanishi#, Hiroyuki Sakurai#, Ken Onodera#, Hisao Kawasaki#, Yoshiharu Takada\* and Kunio Tsuda\*

#Microwave Solid-state Engineering Dept., Komukai Operations, Toshiba Corporation  
1, Komukai-Toshiba-cho, Saiwai-ku, Kawasaki, 212-8581, Japan  
Kazu.taka@toshiba.co.jp

\*Electron Devices Laboratory, Corporate R&D Center, Toshiba Corporation  
1, Komukai-Toshiba-cho, Saiwai-ku, Kawasaki, 212-8581, Japan

**Abstract** — AlGaIn/GaN High Electron Mobility Transistors (HEMTs) were developed for Ka-band. The developed device showed 138 GHz of  $f_{max}$ , which depended on the thickness of the AlGaIn barrier layer and the gate length. It had a 6.4 mm gate periphery on a metal carrier plate. The output power achieved 20 W with impedance matching circuits.

**Index Terms** — AlGaIn, GaN, HEMT, Ka-band.

## I. INTRODUCTION

As a promising candidate for the next generation of microwave power devices, AlGaIn/GaN HEMTs have attracted much research interest due to the inherent advantages of their high breakdown field and high current density. In X-band and Ku-band, AlGaIn/GaN HEMTs have been reported [1, 2] and products using this technology have been released.

In Ku-band, Satellite Communications, SATCOM, has been adopting Solid State Amplifiers, SSPA. In Ka-band, Traveling Wave Tube Amplifiers, TWTA, have been adopted because the output power of GaAs pHEMT is not enough [3, 4].

AlGaIn/GaN HEMTs at millimeter-wave frequencies have drawn a great deal of interest. AlGaIn/GaN HEMTs on-wafer load-pull systems were reported for 5.8 W/mm (5.8 W) at 30GHz with  $10 \times 100 \mu\text{m}$  of the gate width [6], 6.9 W/mm (1.04 W) at 30 GHz with  $2 \times 75 \mu\text{m}$  [10], and 5.4 W/mm (8.05 W) at 30 GHz with 1.5 mm [9]. AlGaIn/GaN HEMTs with impedance matching circuits exhibited 3.3 W/mm (20.7 W) at 26 GHz [15]. AlGaIn/GaN HEMT MMICs were also reported for 3.1 W/mm (5.0 W) at 26.5 GHz with 1.6 mm of the gate width in the final stage, and 3.3 W/mm (4.0 W) at 35 GHz with 1.2 mm of the gate width in the final stage [13, 14].

In this paper, we demonstrate the RF performance of the AlGaIn/GaN HEMTs with impedance matching circuits by comparing the thickness of the AlGaIn barrier layer.

## II. DEVICE STRUCTURE AND FABRICATION

An undoped AlGaIn/GaN HEMT structure was grown on a SiC substrate by MOCVD. As the gate length becomes shorter, the AlGaIn barrier layer thickness should become thinner. Two

types of AlGaIn barrier layers were compared. One had a thickness of  $20\mu\text{m}$  with a 25% Aluminum content. The other one had a  $15\mu\text{m}$  thickness with a 30% Aluminum content. To reduce the short channel current, a GaN buffer layer was important. Three types of GaN buffers were compared. A square shaped Schottky gate electrode was formed with E-beam evaporation. We used SiN film deposited by a conventional PE-CVD for surface passivation. The interconnection, air-bridges and pads were formed with a standard Au-plating process. To know the dependency of the gate length, it was fabricated from  $0.25\mu\text{m}$  to  $0.05\mu\text{m}$ .

## III. DEVICE CHARACTERISTICS

Fig. 1 shows the DC characteristics for the small gate width of the  $100\mu\text{m}$  periphery device. The HEMTs fabricated on the AlGaIn with a thickness of  $15\mu\text{m}$  and a 30% Aluminum content exhibited around  $125\text{mA}/\text{mm}$  of saturation drain current at  $V_{ds}=5\text{V}$ . The pinch-off voltage of all the devices was  $-3\text{V}$ . Maximum transconductance ( $g_m$ ) of  $400\text{mS}/\text{mm}$  was obtained at  $V_{ds}=5\text{V}$ . The HEMT fabricated on the AlGaIn with  $20\mu\text{m}$  of thickness and a 25% Aluminum content exhibited  $115\text{mA}/\text{mm}$  of saturation drain current at  $V_{ds}=5\text{V}$ . The pinch-off voltage was  $-4\text{V}$ . A maximum transconductance ( $g_m$ ) of  $350\text{mS}/\text{mm}$  was obtained at  $V_{ds}=5\text{V}$ .

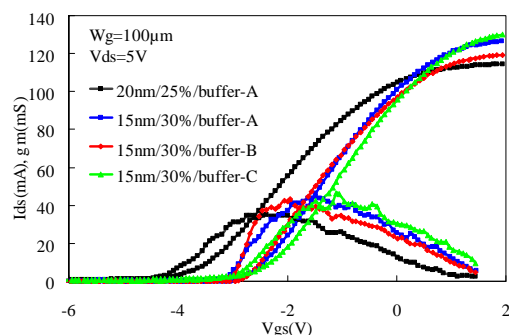


Fig. 1 Measured  $100\mu\text{m}$  AlGaIn/GaN HEMT drain current curves and transfer curves at  $V_{ds}=5\text{V}$ .

Fig. 2 (a) shows the  $f_{max}$  for two fingers of  $50\mu\text{m}$  at  $V_{ds}=24\text{V}$  and  $I_{ds}=16\text{mA}$ . All of the HEMTs, except on buffer-C, increased their  $f_{max}$  along with narrowing the gate length from  $0.25\mu\text{m}$  to  $0.15\mu\text{m}$  and exhibited over  $100\text{GHz}$  of  $f_{max}$ . The HEMT of  $15\text{nm}/30\%/\text{buffer-B}$  showed  $138\text{GHz}$  of  $f_{max}$  at  $0.15\mu\text{m}$  of the gate length. At  $0.05\mu\text{m}$  of the gate length, the  $f_{max}$  was smaller than that at  $0.15\mu\text{m}$  of the gate length. The HEMTs on buffer-C decreased the  $f_{max}$  along with narrowing the gate length from  $0.25\mu\text{m}$  to  $0.05\mu\text{m}$ .

Fig. 2 (b) shows the  $f_{max}$  for two fingers of  $50\mu\text{m}$  at  $V_{ds}=10\text{V}$  and  $I_{ds}=16\text{mA}$ . When comparing  $V_{ds}=24\text{V}$  and  $10\text{V}$ , the decline at  $0.05\mu\text{m}$  of the gate length at  $V_{ds}=10\text{V}$  was smaller than that at  $V_{ds}=24\text{V}$ . That meant that the decline at  $V_{ds}=24\text{V}$  was caused by the short channel effect. The buffer-C did not make enough potential to prevent the short channel effect. Comparing  $20\text{nm}/30\%/\text{buffer-A}$  and  $15\text{nm}/30\%/\text{buffer-A}$ , the decline also depended on the thickness of the AlGaIn barrier layer.

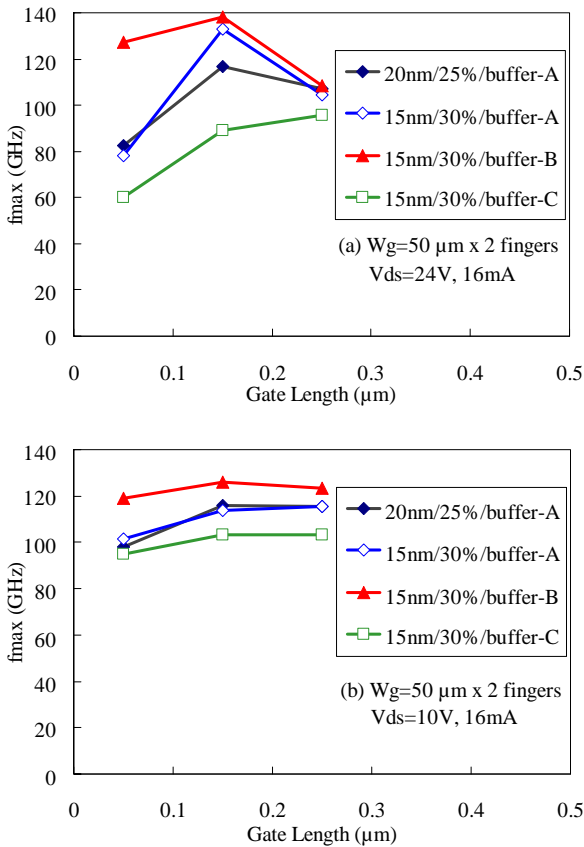


Fig. 2  $f_{max}$  as a function of the gate length for  $50\mu\text{m} \times 2$  devices. (a)  $V_{ds}=24\text{V}$ ,  $16\text{mA}$ , (b)  $V_{ds}=10\text{V}$ ,  $16\text{mA}$

#### IV. OUTPUT POWER PERFORMANCE OF THE UNIT CELLS

Output power densities were measured on a load-pull system to estimate the capability of each structure. The

frequency was set at  $14\text{GHz}$ , which was the frequency at which the tuners in our system could make the optimum impedance for the devices with  $4 \times 100\mu\text{m}$  of the gate width.

The  $15\text{nm}/30\%/\text{buffer-B}$  showed the best  $f_{max}$  of the four, but the power density was the smallest because of current collapse.

Fig.3 shows the operating drain voltage ( $V_{ds}$ ) dependence of 3dB compression output power ( $P_{3dB}$ ) and the power-added efficiency (PAE) of a device which had a gate width of four  $100\mu\text{m}$ -fingers on the  $15\text{nm}/30\%/\text{buffer-A}$  at  $14\text{GHz}$ . The gate length was  $0.15\mu\text{m}$ . These results were measured on a wafer with the source and load conditions tuned to the maximum efficiency for each operating drain voltage. It was noted that the output power increased linearly and the PAE remained constant. These results showed that the structure had a capability of  $2.9\text{W/mm}$  for output power at  $V_{ds}=24\text{V}$ , and  $4.8\text{W/mm}$  for output power at  $V_{ds}=40\text{V}$ .

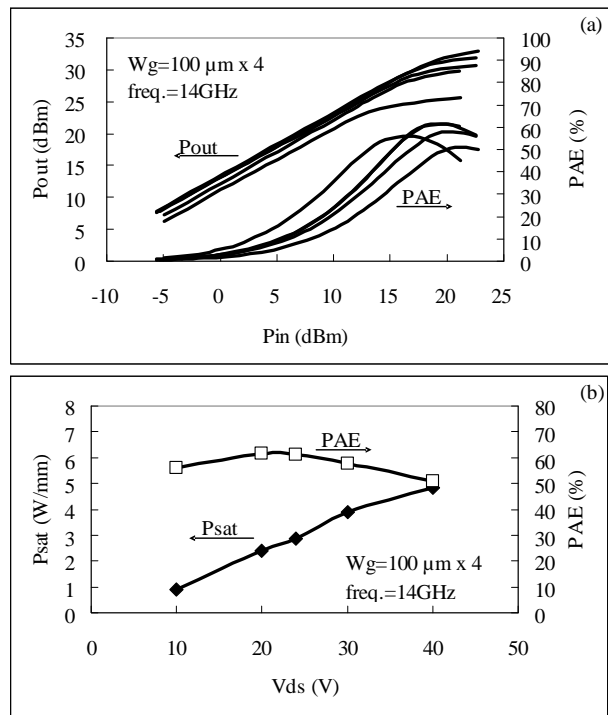


Fig. 3 (a) Output power and power-added efficiency of HEMT on  $15\text{nm}/30\%/\text{buffer-A}$  as a function of input power under CW operating conditions at  $14\text{GHz}$ .  $W_g=100\mu\text{m} \times 4$ , (b) Operating voltage dependence of saturated output power and power-added efficiency under CW operating conditions at  $14\text{GHz}$ .  $W_g=100\mu\text{m} \times 4$ .

The output power density of  $2.9\text{W/mm}$  at  $24\text{V}$  needed  $5.2\text{mm}$  of gate width, which was more than  $104$   $50\mu\text{m}$ -fingers.

Fig. 4 (a) shows MSG/MAG and Mason's U. The number of  $50\mu\text{m}$ -fingers ( $N$ ) was  $2, 4, 8$  and  $12$ . Fig. 4 (b) showed  $f_{max}$  and maximum gain at  $26$  and  $30\text{GHz}$  as a function of the number of  $50\mu\text{m}$ -fingers ( $N$ ). The number of  $50\mu\text{m}$ -fingers for

the unit-cell was determined at twelve by the RF gain and the chip width.

The wafer was thinned to 50 $\mu$ m to reduce the thermal resistance and diced into unit-cells. The unit-cell of  $W_g=0.6$ mm which had twelve 50 $\mu$ m-fingers, was mounted on a metal carrier plate with input and output matching circuits. The matching circuits were tuned at 28GHz for  $V_{ds}=24$ V. Fig. 5 (a) shows the input-output characteristics for  $V_{ds}=24$ V, 30V and 35V. All of the output powers and gains were almost the same. Fig. 5 (b) shows the output power and PAE as a function of  $V_{ds}$ . Because the matching circuits were fixed, the output power didn't increase with the drain voltage as it had done when the measurement was set at 14GHz on a wafer with sourcepull and loadpull tuners. The saturated output power was 3.6W/mm for  $V_{ds}=24$ V at 28GHz. The PAE was 28.6%.

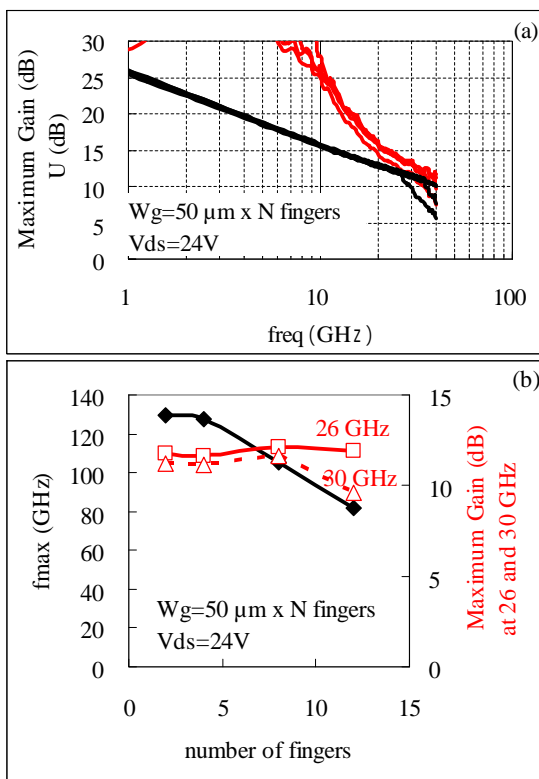


Fig. 4 (a) MSG/MAG and Mason's U. The number of 50 $\mu$ m-fingers (N) were 2, 4, 8 and 12, (b)  $f_{max}$  and maximum gain at 26 and 30GHz as a function of the number of 50 $\mu$ m-fingers (N).

#### V. OUTPUT POWER PERFORMANCE OF A 6.4-MM-WIDE DEVICE

Fig. 6 shows the input-output characteristics of a 16-cell HEMT on a metal carrier plate with input and output matching circuits for  $V_{ds}=24$ V at 26GHz. The measured output power reached 15W (41.7dBm) at a drain voltage of 24V. The maximum PAE was 13.3% with 9W of output power.

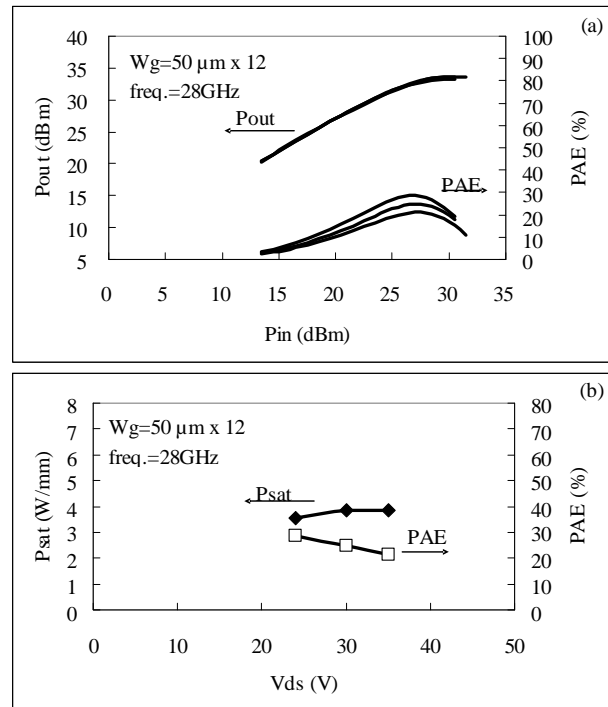


Fig. 5 (a) Input-output characteristics of a unit-cell HEMT on a metal carrier plate with input and output matching circuits for  $V_{ds}=24$ V, 30V and 35V at 28GHz. (b) Output power and PAE as a function of  $V_{ds}$ .

Fig. 7(a) shows the saturated output power for AlGaIn/GaN HEMT reported as a function of the operating frequency. To the best of our knowledge, the saturated output power of over 20W under CW operation in Ka-band is the top level. Fig.7 (b) shows the power added efficiency for AlGaIn/GaN HEMT reported in Ka-band as a function of the saturated output power. To the best of our knowledge, the power added efficiency of 18.5% with the saturated output power of 20W in Ka-band is the top level.

#### VI. CONCLUSION

In this study, we developed AlGaIn/GaN HEMTs for Ka-band by optimizing the AlGaIn thickness and aluminum content. We showed the gate length dependency of  $f_{max}$  for some AlGaIn barrier layers. The output power density and output power of the unit-cell on the AlGaIn with a thickness of 15 $\mu$ m and a 30% Aluminum content were 3.6 W/mm and 2.1W. The HEMT with a gate width of 6.4mm demonstrated a saturated output power of 20W under CW operating conditions at 26GHz. This is our first step in developing GaN MMIC for Ka-band.

## REFERENCES

- [1] K. Takagi, S. Takatsuka, Y. Kashiwabara, S. Teramoto, K. Matsushita, H. Sakurai, K. Onodera, H. Kawasaki, Y. Takada, K. Tsuda, "Ku-Band AlGaIn/GaN-HEMT with over 30% of PAE", 2009 IEEE MTT-S Int. Microwave Symp., Dig., pp. 457-460, June 2009.
- [2] H. Shigematsu, Y. Inoue, A. Akasegawa, M. Yamada, S. Masuda, Y. Kamada, A. Yamada, M. Kanamura, T. Ohki, K. Makiyama, N. Okamoto, K. Imanishi, T. Kikkawa, K. Joshin, and N. Hara, "C-band 340-W and X-band 100-W GaN Power Amplifiers with Over 50-% PAE", 2009
- [3] M. R. Lyons, C. D. Grondahl and S. M. Daoud, "Design of Low-Cost 4W & 6W MMIC High Power Amplifiers for Ka-Band Modules", 2004 IEEE MTT-S Dig., 2004, pp.1673-1676.
- [4] Kris (Keon-Shik) Kong, Bruce Nguyen, Sabyasachi Nayak, and Ming-Yih Kao, "Ka-Band MMIC High Power Amplifier (4W at 30 GHz) with Record Compact Size", 2005 IEEE CSIC Symp. Digest, pp232-235
- [5] Y.-F. Wu, M. Moore, et.al., "3.5-Watt AlGaIn/GaN HEMTs and Amplifiers at 35 GHz", 2003 IEEE Int. Electron Device Meeting. Dig., pp. 579-581, December 2003.
- [6] T. Inoue, Y. Ando, H. Miyamoto, and Y. Okamoto, et.al., "30GHz-band 5.8W High-Power AlGaIn/GaN Heterojunction-FET", 2004 IEEE MTT-S Int. Microwave Symp. Dig., pp.1649-1652, June 2004.
- [7] M. Micovic, et.al., "Ka-band MMIC Power Amplifier in GaN HFET Technology", 2004 IEEE MTT-S Int. Microwave Symp., Dig., pp. 1653-1656, June 2004.
- [8] M. Micovic, A. Kurdoghlian, H. P. Moyer, P. Hashimoto, A. Schmitz, I. Milosavljevic, P. J. Willadsen, W.-S. Wong, J. Duvall, M. Hu, M. Wetzler, D. H. Chow, "GaN MMIC Technology for Microwave and Millimeter-wave Applications", 2005 IEEE CSIC Symp. Digest, pp173-176
- [9] Y. -F. Wu, M. Moor, A. Saxler, T. Wisleder, U. K. Mishra and P. Parikh, "8-Watt GaN HEMTs at Millimeter-Wave Frequencies", 2005 IEEE IEDM Tech. Dig., December 2005, pp. 593-595.
- [10] J. S. Moon, Shihchang Wu, D. Wong, I. Milosavljevic, A. Conway, P. Hashimoto, M. Hu, M. Antcliffe, and M. Micovic, "Gate-Recessed AlGaIn-GaN HEMTs for High-Performance Millimeter-Wave Applications", IEEE Electron Device Lett., 2005, 26, No.6, pp. 348-350.
- [11] M. van Heijningen, and F. van Raay, et.al., "Ka-Band AlGaIn/GaN HEMT High Power and Driver Amplifier MMICs", 13th GAAS Symp. Proceedings, Paris, France, October 2005, pp237-240
- [12] K. S. Boutros, et.al., "5W GaN MMIC for Millimeter-Wave Applications", 2006 IEEE CSIC Symp., pp93-95, Nov. 2006.
- [13] A. M. Darwish, et.al., "4-Watt Ka-Band AlGaIn/GaN Power Amplifier MMIC", 2006 IEEE MTT-S Int. Microwave Symp., Dig., pp. 726-729, June 2006.
- [14] A. M. Darwish, K. Boutros, B. Luo, B. D. Huebschman, E. Viveiros, and H. A. Hung, "AlGaIn/GaN Ka-Band 5-W MMIC Amplifier", IEEE Trans. Microw. Theory Tech., 54, no. 12, pp.4456-4463, Dec. 2006.
- [15] Y. Murase, A. Wakejima, et.al., "CW 20-W AlGaIn/GaN FET Power Amplifier for Quasi-Millimeter Wave Applications", 2007 IEEE CSIC Symp., pp36-39, Oct. 2007.

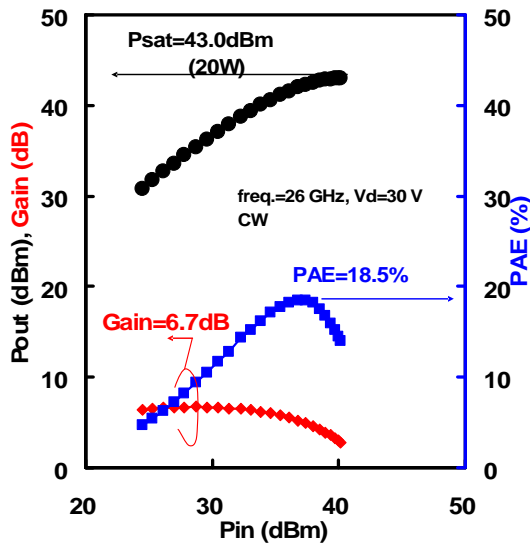


Fig. 6 Input-output characteristics of a 16-cell HEMT on a metal carrier plate with input and output matching circuits for  $V_{ds}=24V$  at 26GHz.

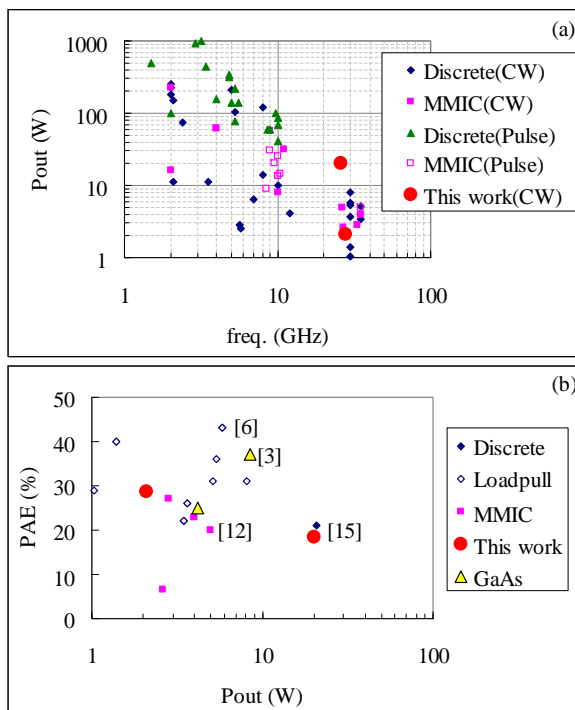


Fig. 7 (a) Power performance of AlGaIn/GaN HEMT developed in this work and the works previously reported. (b) PAE performance of AlGaIn/GaN HEMT developed in this work and the works previously reported at Ka-band.

### IEEE

Copyright c 1999-2010 IEEE. Personal use of this material is permitted. However, permission to reprint/republish this material for advertising or promotional purposes or for creating new collective works for resale or redistribution to servers or lists, or to reuse any copyrighted component of this work in other works must be obtained from the IEEE.

This material is presented to ensure timely dissemination of scholarly and technical work. Copyright and all rights therein are retained by authors or by other copyright holders. All persons copying this information are expected to adhere to the terms and constraints invoked by each author's copyright. In most cases, these works may not be reposted without the explicit permission of the copyright holder.